Optical absorption and localized electronic states in amorphous $CsPbX_3$, PbX_2 and TlX (X = Cl, Br)

1999 J. Phys.: Condens. Matter 11 8155

(http://iopscience.iop.org/0953-8984/11/41/318)

J. Phys.: Condens. Matter **11** (1999) 8155–8162. Printed in the UK PII: S0953-8984(99)03715-7

Optical absorption and localized electronic states in amorphous $CsPbX_3$, PbX_2 and TlX (X = Cl, Br)

S Kondo, H Tanaka and T Saito

Research Centre of Development of the Far-Infrared Region, Fukui University, Bunkyo, Fukui 910-0017, Japan

Received 26 April 1999

Abstract. Systematic comparison of the absorption spectra in the amorphous state has been made between ionic compounds ($CsPbX_3$, TlX and PbX_2 with X = Br and Cl) containing $6s^2$ ions as a constituent. The spectra exhibit several common features including nearly the same optical energy gap observed for all the compounds with the same X, despite the largely different spectral outline in their crystalline state. The common features are related to strong localization of the one-electron states of the $6s^2$ ions. In contrast to the case of covalent semiconductors, the introduction of the long-range order due to crystallization gives rise to a significant change of the density of states related to the $6s^2$ ions.

1. Introduction

Optical properties of TlX, $CsPbX_3$ and PbX_2 (X = Cl, Br) are characterized by a dominant contribution of the $6s^2$ ions (Tl^+ and Pb^{2+}) to low-energy fundamental absorption. In TlX, which crystallizes in the CsCl structure, the Tl^+ 6s and 6p orbitals give a direct contribution to the absorption spectrum near the fundamental edge together with X^- 3p or 4p orbitals, exhibiting a sharp cationic exciton peak [1]. Energy band calculations [2–6] indeed show that upper valence bands are constructed from the Tl^+ 6s and X^- 3p or 4p orbitals, and lower conduction bands from the Tl^+ 6p orbitals; a cationic direct energy gap, responsible for the (direct) exciton peak, is located at the X point due to positive and negative k dispersions of the uppermost valence and lowermost conduction bands, respectively, along the Γ–X direction.

In $CsPbX_3$, which crystallize in a slightly distorted perovskite structure, optical properties are governed by the octahedral quasicomplex $Pb^{2+}(X^-)_6$ embedded in a simple cubic matrix of Cs^+ ions. The six X^- ions are located at the face-centred positions of the cube and the cation Pb^{2+} is at the cube centre. Heidrich *et al* [7, 8] have calculated the band structure of the compounds based on the empirical LCAO (linear combination of atomic orbitals) method. They show that the band structure of $CsPbX_3$ is very similar in feature to that of TlX on account of (nearly) the same simple cubic space group of the two compounds as well as of the same $6s^2$ configuration of the cation. Both the Pb^{2+} 6s and X^- 3p or 4p orbitals merge into upper valence bands and the Pb^{2+} 6p orbitals take part in lower conduction bands. The only notable difference (from TlX), which comes from the difference in the coordination number for the central cation, is that a cationic direct gap is located at the R point (instead of the X point in TlX) because of larger positive and negative k dispersions of the uppermost valence and lowermost conduction bands, respectively, along the Γ–R direction rather than along the Γ–X direction. The intervening Cs^+ ions in $CsPbX_3$ only contribute their 6s orbitals to much higher conduction

0953-8984/99/418155+08$30.00

bands. The low-energy optical absorption [7–10] and reflection [7, 8, 11–13] spectra, which are characterized by a sharp cationic direct exciton (R-point exciton) peak, have indeed been well explained in the framework of this band structure.

As for PbX_2, which have an orthorhombic structure with the Pb^{2+} ion surrounded by nine X^- ions, there have been only experimental studies in the literature; the fundamental absorption near the edge is dominated by Pb^{2+} 6s to 6p transitions also exhibiting a sharp cationic exciton peak [11–19].

All the compounds mentioned above can be made amorphous by quench deposition yielding film samples. The amorphous films of these compounds all exhibit excellent transmittances below the absorption edges and have well defined, characteristic crystallization temperatures (302 K for $CsPbCl_3$ [20], 296 K for $CsPbBr_3$ [20], 98 K for TlCl [21], 94 K for TlBr [22], 281.5 K for $PbCl_2$ [23] and 335 K for $PbBr_2$ [24]) at which their absorption spectra drastically change in outline.

Recently we showed [20] that amorphous $CsPbCl_3$ and $CsPbBr_3$ are characterized by strongly reduced optical absorption (compared to that of crystalline $CsPbX_3$) over a few electron volts of photon energy above the fundamental edge and exhibit a large blue shift of the optical energy gap. An explanation for these characteristics is given based on the assumption that all the Pb^{2+} 6s and 6p states are localized by amorphization together with appreciable parts of X^- 3p or 4p states (see section 3). Concerning other $6s^2$-ion halides mentioned above, however, the studies of the amorphous films have mainly been aimed at their optical characterization, and little has been explored concerning the spectral assignment and the associated electronic states of the amorphous films.

In view of the close similarity in the behaviour of the $6s^2$ ions in $CsPbX_3$, TlX and PbX_2 (that is, the $6s^2$ ions make a dominant contribution to low-energy fundamental absorption, or to electronic energy band structure near the band gap), systematic consideration of amorphization-induced spectral change of these compounds would lead to a new understanding of the amorphous state of ionic compounds. This stimulated the present study. Thus, we will first provide a full set of the fundamental absorption spectra, up to 6.2 eV, of the compounds both for the amorphous and the crystalline (crystallized) films in order to extract (in section 2) the spectral characteristics (similarities and differences) from the viewpoint of comparative investigation. This enables a thorough discussion (in section 3) on the nature of optical absorption and related electronic states for the amorphous state of these compounds, to clarify correlative electronic properties in the amorphous state of this particular group of ionic compounds.

2. Spectral characteristics

Figures 1 and 2 summarize the comparison of the fundamental absorption spectra at 77 K between amorphous (curves a) and crystalline (curves c) films for chlorides (X = Cl, figure 1) and bromides (X = Br, figure 2). The amorphous films were all achieved by quench deposition onto 77 K substrates and the crystalline ones were produced via the crystallization of the same (amorphous) films (the details are given in, for example, [22]). The spectral structures of the crystalline films resemble those of polycrystalline films reported for the respective compounds (for example, [1] for TlX, [8] for $CsPbX_3$ and [16] for PbX_2; absorption spectra of single crystalline films are not available).

We first describe the spectral-structure assignment available for the crystalline films to exemplify the dominant contribution of the $6s^2$ cations to low-energy structures. In crystalline (c-) $CsPbX_3$, the low-energy structures occur at the R or X point in the Brillouin zone [7, 8], i.e. peak 1 at R, peak 2 at X, both arising from the 6s to 6p transition in the Pb^{2+}-ion sublattice, and

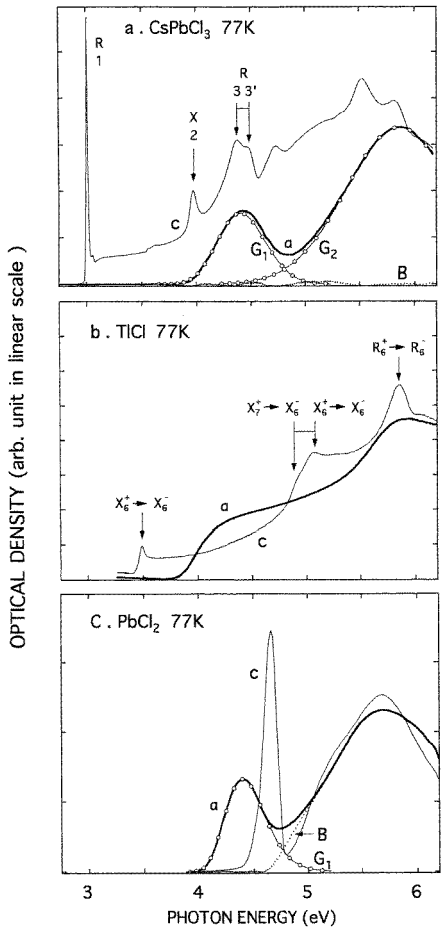

Figure 1. Amorphous versus crystalline—their fundamental absorption spectra at 77 K compared between (a) $CsPbCl_3$, (b) TlCl and (c) $PbCl_2$. The measurements were first made on the amorphous films (spectra a) and then the films were crystallized to measure spectra c. In (a), spectrum a is decomposed into two weakly asymmetric Gaussian bands, G_1 and G_2, with the remainder (a minus G_1 minus G_2) as the background absorption, B. In (c), spectrum a is decomposed into a skewed Gaussian band, G_1, and the background absorption, B.

doublet 3 and 3′ at R due to charge-transfer transitions from X^- 3p- or 4p-like valence to Pb^{2+} 6p-like conduction bands. The doublet structure arises from halogen p spin–orbit interaction. The spectra of c-TlX are composed of the first peak due to Tl^+ 6s-to-6p transitions and the doublet of a charge-transfer type (from spin–orbit split X^- 3p or 4p to Tl^+ 6p), both occurring at X. These structures correspond to the R-point structures of c-$CsPbX_3$; the alternation of the critical points (X for c-TlX instead of R for c-$CsPbX_3$) stems from the difference in the coordination number for the cations. The fourth peak in c-TlX is again due to Tl^+ 6s-to-6p transitions and has the same critical-point origin as peak 1 of c-$CsPbX_3$ (conversely, the first peak in c-TlX has the same critical-point origin as peak 2 of c-$CsPbX_3$). In c-PbX_2, although no critical-point assignment is available in the literature, many experimentalists (see, for example, [18]) have attributed the first peak to cationic exciton due to $6s^2$-to-6s6p excitation in the Pb^{2+}-ion sublattice. According to [14], the strong absorption extending to higher energies in c-$PbCl_2$

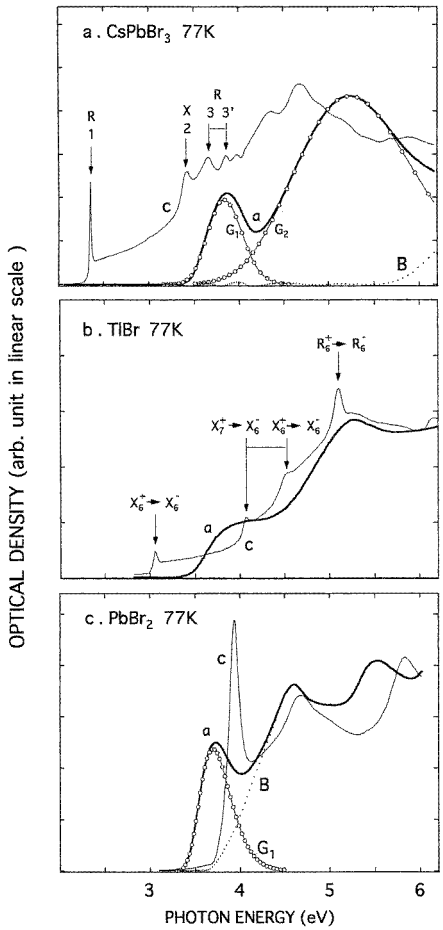

Figure 2. As for chlorides (X = Br) in figure 1 but for bromides (X = Cl).

and the band around 4.6 eV in c-$PbBr_2$ are associated with charge-transfer transitions from X^- 3p or 4p to Pb^{2+} 6p states, and the band around 5.8 eV in c-$PbBr_2$ is attributed to intra-cationic transitions.

When the compounds are amorphized, appreciable change in the spectra occurs depending on the different types of compound. In amorphous (a-) $CsPbX_3$, the fine structures that exist in the crystalline state are all absent, leaving behind the two broad bands, around 4.4 and 5.8 eV for a-$CsPbCl_3$ and around 3.8 and 5.2 eV for a-$CsPbBr_3$. It is difficult to find global similarity in the spectral outline between c- and a-$CsPbX_3$. Further, the amorphization accompanies significant reduction in the integrated absorption intensity, by a factor of about 2 for X = Cl and about 1.6 for X = Br in the measured region up to 6.2 eV. Amorphization of TlX is also characterized by the disappearance of fine structures including a missing excitonic peak. The spectra are outlined with the two broad bands, around 4.3 and 5.8 eV for a-TlCl and around 3.9 and 5.2 eV for a-TlBr, somewhat similar to the case of a-$CsPbX_3$. It is, however, noted that there is global similarity in the spectral outline between c- and a-TlX. In fact the integrated absorption intensity was shown to be almost the same. In PbX_2, all the main structures of the crystalline state still exist in the amorphous state (the integrated absorption intensity was

almost the same for the two states). In particular, the first bands around 4.4 eV for a-$PbCl_2$ and 3.7 eV for a-$PbBr_2$ correspond to the amorphous counterparts of the cationic exciton peaks.

Notably, each type of compound shows a characteristic shift of optical energy gap on amorphization, i.e. a blue shift by as much as ∼1 eV for $CsPbX_3$ and by ∼0.5 eV for TlX, while a red shift by ∼0.3 to 0.4 eV for PbX_2. Further, the resulting (Tauc) optical energy gaps in the amorphous state are nearly the same for all three types of compound, giving values of ∼3.9 eV for X = Cl and ∼3.4 eV for X = Br.

The spectra of a-$CsPbX_3$ are decomposed into two (weakly skewed) Gaussian functions, G_1 and G_2, as demonstrated in [20]. (The peak energies of G_1 and G_2 are close to those of A and C bands [25], respectively, of Pb-doped alkali halides). Decomposition can also be made for the first bands of a-PbX_2, yielding a (weakly skewed) Gaussian band (curves G_1) separated from high-energy parts (curves B). We note that the crystalline courterpart of this band, namely the exciton band of c-PbX_2, can be fitted by multiple Lorentzian functions and that the integrated absorption intensities of the Gaussian and the multiple Lorentzians are nearly the same.

The energy parameters of the spectral decomposition are summarized in table 1, together with the associated energies of a-TlX and the optical energy gaps E_g of all the amorphous compounds.

Table 1. The peak energies (E_1, E_2) and their difference ($E_2 - E_1$) for G_1 and G_2 bands of a-$CsPbX_3$ from [20], the peak energy (E_1) for the G_1 band of a-PbX_2 and the optical energy gaps E_g of a-$CsPbX_3$, a-TlX and a-PbX_2 (X = Cl, Br), all given in units of electron volts. The energy locations (E_1, E_2) and their differences ($E_2 - E_1$) of the first and second bands of a-TlX are also listed in parentheses.

	E_1	E_2	$E_2 - E_1$	E_g
a-$CsPbCl_3$	4.406	5.866	1.460	3.9
a-TlCl	(4.3)	(5.8)	(1.5)	3.8
a-$PbCl_2$	4.418			4.0
a-$CsPbBr_3$	3.843	5.241	1.398	3.4
a-TlBr	(3.9)	(5.2)	(1.3)	3.4
a-$PbBr_2$	3.700			3.4

3. Discussion

It is convenient to summarize the previous explanation for $CsPbX_3$ discussed in [20] to provide a starting point for a systematic interpretation of the spectral characteristics extracted in section 2. The basic idea is illustrated by figure 3 (left part): the prototype of the one-electron energy states of $CsPbX_3$ is given based on the MO (molecular orbital) theory applied to the octahedral $Pb^{2+}(X^-)_6$ quasicomplex of O_h symmetry. Of the nine MOs (constructed from the 6s and 6p states of the central Pb^{2+} ion and the 3p or 4p states of the six ligand X^- ions), the upper three, namely, unoccupied t^a_{1u}, highest occupied a^a_{1g} and second highest occupied e^n_g, are of utmost concern with the spectral behaviour described in section 2 (the superscripts a, b and n denote antibonding, bonding and nonbonding orbitals, respectively). Since t^a_{1u} and a^a_{1g} are composed mainly of Pb^{2+} 6s and 6p states, respectively, they are represented by the atomic quantum number j, i.e. the spin–orbit split $j = 3/2$ and $1/2$ states for t^a_{1u} and the $j = 1/2$ state for a^a_{1g}. In c-$CsPbX_3$, t^a_{1u} merges into lower conduction bands, a^a_{1g} and e^n_g into upper valence bands (other MOs contribute to deeper valence bands). When the crystal is amorphized, these extended states all converge to own localized states with particular eigenenergies, as shown in

the figure. G_1 and G_2 bands of a-$CsPbX_3$ are the transitions from the filled $j = 1/2$ localized state to the empty $j = 1/2$ and 3/2 localized states, respectively (their energy separations, $E_2 - E_1$ in table 1 are close to the Pb 6p spin–orbit splitting energy, 1.3 eV [26]). Charge-transfer transitions from the e_g^n localized states to the empty localized states occur at high energies above the G_1 and G_2 bands. Thus, figure 3 (left part) gives an explanation of the amorphization-induced spectral change of $CsPbX_3$, i.e. the large blue shift ($\sim$1 eV) of the absorption edge and the significant reduction in the integrated absorption intensity, yielding the two Gaussian bands.

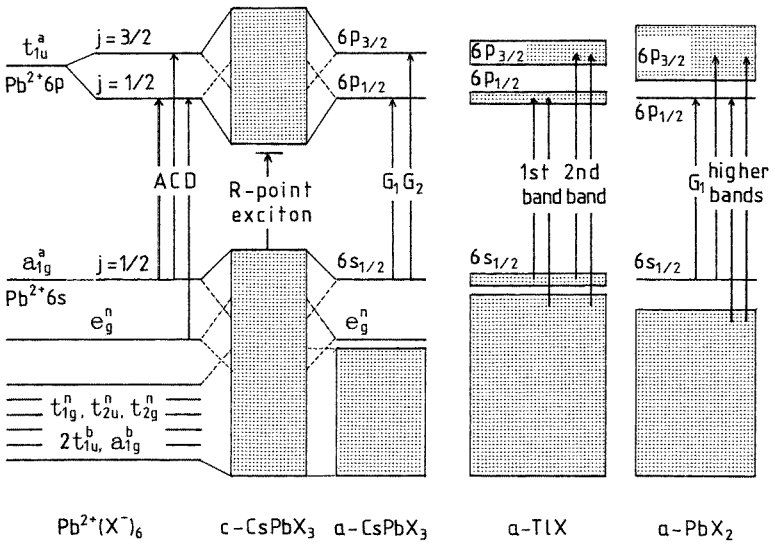

Figure 3. A schematic energy band diagram for a-$CsPbX_3$, a-TlX and a-PbX_2 (X = Cl, Br) illustrating amorphization-induced localization of the associated one-electron states (see the text).

Considerations analogous to those above may also be applicable to TlX with some modification, in view of the similar energy band structure. In particular, the spectral two-band feature of a-TlX provides a measure of the localized nature of the Tl^+ 6s and 6p states. It is probable that the conduction states coming from t_{1u}^a and upper valence states from a_{1g}^a are more or less localized by amorphization leading to a tendency to form spin–orbit split $j = 1/2$ and 3/2 states for t_{1u}^a and $j = 1/2$ state for a_{1g}^a, as shown in the right part of figure 3; the spectral two-band feature corresponds to two transitions, from the filled $j = 1/2$ to empty $j = 1/2$ and 3/2 states. The energy separation between the two bands, $\sim$1.5 eV for a-TlCl and $\sim$1.3 eV for a-TlBr, is indeed comparable to the Tl 6p spin–orbit splitting energy, 1.41 eV [4]. However, the localized nature of the associated one-electron states is considered to be much weaker, particularly in the $j = 3/2$ states, than the case of $CsPbX_3$, since the two bands for a-TlX are by no means shaped like Gaussians. On the other hand, valence states from e_g^n are, in great contrast to the case of $CsPbX_3$, expected to be little localized by amorphization, with their energies showing upward k dispersion along the Γ–X direction in the Brillouin zone. This accounts for the smaller blue shift of the optical energy gap than the a-$CsPbX_3$ case. The optical transitions from these extended states to the empty $j = 1/2$ and 3/2 states may have the effect to further obscure the two bands, thus resulting in absorption spectra similar in gross features to those of c-TlX.

As mentioned in section 1, the quasicomplexes in $CsPbX_3$ are embedded in the cubic Cs^+-ion matrix. Therefore, the stronger localization of electronic states for Pb^{2+} ions in a-$CsPbX_3$ than those for Tl^+ ions in a-TlX is considered to be due to intervening Cs^+ ions in the former. It is interesting that the dilution of the Pb^{2+} ions by the Cs^+ ions in an otherwise similar configuration leads to weaker dispersion of the X^- 3p or 4p orbitals (e_g^n) and reduction of their coupling to the Pb^{2+} 6s orbitals.

In PbX_2, upper valence bands may be constructed from Pb^{2+} 6s and X^- 3p or 4p orbitals and lower conduction bands from Pb^{2+} 6p orbitals as in the cases of $CsPbX_3$ and TlX. The Gaussian band in a-PbX_2 is considered to have very similar origin to that of the G_1 band of a-$CsPbX_3$, suggesting that both the Pb^{2+} 6s state contributing to upper valence bands and the Pb^{2+} $6p_{1/2}$ state contributing to the lowest conduction band are localized by amorphization; the Gaussian band can be assigned as due to localized transitions from the filled 6s to the empty $6p_{1/2}$ states within the Pb^{2+} ions as shown in figure 3 (right part). It is likely that, by amorphization, all the extended states contributing to the c-phase excitonic transitions are localized and take part in the localized absorption responsible for the Gaussian band, in view of the near equality in the integrated absorption intensity between the Gaussian and the exciton absorption (multiple Lorentzians). Concerning the high-energy absorption above the Gaussian band, where the absorption spectra of a-PbX_2 and c-PbX_2 are very similar in features to each other, the optical transitions are considered to be related to extended states, as shown in the figure.

It is interesting to note that the exciton absorption for PbX_2 is changed to localized absorption of a nonexcitonic nature by amorphization, in great contrast to the cases of $CsPbX_3$ and TlX, in which no amorphous counterpart of the exciton absorption is observed in the amorphous state. Although the exciton absorptions for these compounds are all based on intracationic transitions in the $6s^2$-ion sublattice, two different types of exciton have been assigned, namely, the Wannier exciton for $CsPbX_3$ [10, 13] and TlX [1], and the Frenkel exciton for PbX_2 [18]. The Wannier exciton is a coupled effective mass state of the 6s-like valence (hole) and the $6p_{1/2}$-like conduction (electron) states. Since these extended states are localized by amorphization such an exciton cannot be formed in a-$CsPbX_3$ and a-TlX. On the other hand, the Frenkel exciton for PbX_2 is basically an excitation of a single Pb^{2+} ion, which moves from ion to ion on the Pb^{2+}-ion sublattice. Such an excited state of the Pb^{2+} ion is also possible for a-PbX_2 though it can no longer move. This corresponds to the amorphous counterpart of the exciton state.

The amorphous states of $CsPbX_3$, TlX and PbX_2 have the common property that the 6s and $6p_{1/2}$ states of the $6s^2$ ions are localized. Furthermore, the 6s to $6p_{1/2}$ promotion energies are nearly the same for the three $6s^2$ ions embedded in different amorphous surroundings, leading to nearly the same energy location of the first band (E_1 in table 1) and nearly the same optical energy gap (E_g in table 1). Such common features for the $6s^2$ ions are, however, absent from the crystalline state; on crystallization, both the 6s and $6p_{1/2}$ states merge into extended states, giving rise to their energetic dispersion in the Brillouin zone. As a result, band gaps smaller or larger than the amorphous-state optical energy gaps occur in a way strongly dependent on the resulting crystal structure; the established long-range order plays an important role in determining the DOS (density of states) function (compared to the case of covalent semiconductors), probably due to the long-range nature of the ionic potential in the crystal. For c-$CsPbX_3$ and c-TlX, the large band dispersion leads to a large red shift of the optical energy gap, while for c-PbX_2 a (probably) small band dispersion results in the blue shift. The blue shift for c-PbX_2 is considered to be caused by the reduction of Coulomb and exchange interactions between the $6p_{1/2}$ electron and the 6s hole, since the electron and the hole have a possibility to be more or less distant in position from each other in the exciton states.

Finally, mention should be made of the old finding (empirical rule) that in covalent semiconductors, including both tetrahedral and chalcogenide semiconductors, amorphization has the effect of reducing the differences between their optical energy gaps [27]. This has been explained in terms of strengthening of the covalent character of the bond. The empirical rule holds also for the ionic compounds investigated above, though the main cause of the amorphization-induced shift of the gaps is the strengthening of the ionic, instead of covalent, character.

Acknowledgments

This work was partly supported by The Hokuriku Industrial Advancement Centre and partly by a Grant-in-Aid for Scientific Research from the Ministry of Education, Science, Sports and Culture in Japan.

References

[1] See, for example, Bachrach R Z and Brown F G 1970 *Phys. Rev.* B **1** 818
[2] Inoue M and Okazaki M 1971 *J. Phys. Soc. Japan* **31** 1313
[3] Overhof H and Treusch J 1971 *Solid State Commun.* **9** 53
[4] Overton J and Hernandez J P 1973 *Phys. Rev.* B **7** 778
[5] Treusch J 1975 *Phys. Rev. Lett.* **34** 1343
[6] Van Dyke J P and Samara G A 1975 *Phys. Rev.* B **11** 4935
[7] Heidrich K, Künzel H and Treusch J 1978 *Solid State Commun.* **25** 887
[8] Heidrich K, Schäfer W, Schreiber M, Söchtig J, Trendel G and Treusch J 1981 *Phys. Rev.* B **24** 5642
[9] Ito H, Onuki H and Onaka R 1978 *J. Phys. Soc. Japan* **45** 2043
[10] Fröhlich D, Heidrich K, Künzel H, Trendel F and Treusch J 1979 *J. Lumin.* **18/19** 385
[11] Belikovich B A, Pashchuk I P and Pidzyrailo N S 1977 *Opt. Spectrosc.* **42** 62
[12] Amitin L N, Anistratov A T and Kuznetsov A I 1979 *Sov. Phys.–Solid State* **21** 2041
[13] Pashuk I P, Pidzyrailo N S and Matsko M G *Sov. Phys.–Solid State* **23** 1263
[14] De Gruijter W C 1973 *J. Solid State Chem.* **6** 151
[15] Malysheva A F and Plekhanov V G 1973 *Opt. Spectrosc.* **34** 302
[16] Plekhanov V G 1973 *Phys. Status Solidi* b **57** K55
[17] Eijkelenkamp A J H and Vos K 1976 *Phys. Status Solidi* b **76** 769
[18] Fujita M, Nakagawa H, Fukui K, Matsumoto H, Miyanaga T and Watanabe M 1991 *J. Phys. Soc. Japan* **60** 4393
[19] Kanbe J, Takezoe H and Onaka R 1976 *J. Phys. Soc. Japan* **41** 942
[20] Kondo S, Sakai T, Tanaka H and Saito T 1998 *Phys. Rev.* B **58** 11 401
[21] Kondo S, Itoh T, Saito T and Mekata M 1991 *Solid State Commun.* **78** 557
[22] Kondo S, Itoh T, Saito T and Mekata M 1991 *J. Phys. Soc. Japan* **60** 2764
[23] Kondo S, Maruyama H and Saito T 1995 *Phys. Status Solidi* a **147** 453
[24] Kondo S, Arakawa T and Saito T 1993 *Japan. J. Appl. Phys.* 1 **32** 4511
[25] Radhakrishna S and Pande K P 1973 *Phys. Rev.* B **7** 424
[26] Amitin L N, Anistratov A T and Kuznetsov A I 1979 *Sov. Phys.–Solid State* **20** 2041
[27] Vorlicek V 1975 *Czech. J. Phys.* B **25** 1042